PNAS RESEARCH ARTICLE | ECOLOGY

Constraining nonlinear time series modeling with the metabolic theory of ecology

Stephan B. Munch[a,b,1], Tanya L. Rogers[a], Celia C. Symons[c], David Anderson[d], and Frank Pennekamp[e,1]

Edited by Nils Stenseth, University of Oslo, Oslo, Norway; received July 8, 2022; accepted February 8, 2023

Forecasting the response of ecological systems to environmental change is a critical challenge for sustainable management. The metabolic theory of ecology (MTE) posits scaling of biological rates with temperature, but it has had limited application to population dynamic forecasting. Here we use the temperature dependence of the MTE to constrain empirical dynamic modeling (EDM), an equation-free nonlinear machine learning approach for forecasting. By rescaling time with temperature and modeling dynamics on a "metabolic time step," our method (MTE-EDM) improved forecast accuracy in 18 of 19 empirical ectotherm time series (by 19% on average), with the largest gains in more seasonal environments. MTE-EDM assumes that temperature affects only the rate, rather than the form, of population dynamics, and that interacting species have approximately similar temperature dependence. A review of laboratory studies suggests these assumptions are reasonable, at least approximately, though not for all ecological systems. Our approach highlights how to combine modern data-driven forecasting techniques with ecological theory and mechanistic understanding to predict the response of complex ecosystems to temperature variability and trends.

population dynamics | thermal biology | empirical dynamic modeling | physical–biological interactions

Forecasting the dynamics of ecosystems is a major challenge (1, 2), yet critical for the effective management of natural resources (3). More powerful methods, the increasing scale and resolution of ecological datasets, and advances in ecological theory can improve our ability to accurately forecast ecological systems, especially over the short term relevant for environmental decision-making (1). However, the complexity of natural ecosystems and the influence of numerous environmental drivers still pose a significant challenge to ecosystem forecasting, particularly in the face of ongoing environmental change (2).

Data-driven techniques such as machine learning have revolutionized forecasts of dynamical systems (4). However, a major drawback of these techniques is their limited ability to extrapolate to new conditions, as purely data-driven techniques perform poorly outside the historic envelope of variation (5). In contrast, mechanistic models can deal with changing conditions because they rely on mechanism, rather than past behavior, to extrapolate to previously unobserved conditions (6). Combining data-driven techniques with process-based models that obey mechanistic constraints could lead to better predictions of ecosystem dynamics. Blended models combine artificial intelligence and machine learning (e.g., deep neural networks) with process-based models to represent complex, integrated systems with many components and biophysical constraints (7). Thus, blended modeling approaches improve extrapolation by restricting data-driven predictions to those that follow physical laws (7). The potential for blending data-driven and process-based forecasting has been recognized across various fields, including earth system science and medicine (8, 9), suggesting applications of this growing research area for ecology.

Empirical dynamic modeling (EDM) is a data-driven machine learning technique that has shown great promise in forecasting the dynamics of complex ecosystems (10, 11). The foundation of EDM is Takens' embedding theorem which states that lags of a single time series can reconstruct the dynamics of the complex, multidimensional system from which that series originated (12). Predictions are made by following nearby states (in delay coordinate space) forward in time, assuming that the past behavior of nearby states will reflect the future behavior of the system. EDM has been used successfully in many ecological applications where mechanistic models were lacking (11, 13, 14), and sometimes can even outperform forecasts made by fitting the "correct" underlying mechanistic model (13). However, the fact that EDM does not require mechanism may also be a weakness—physical laws do not constrain its predictions, potentially resulting in implausible ecological states. Blending the EDM approach with first principles and biophysical constraints could improve forecasts.

Significance

Forecasting how populations respond to climate change is an important challenge for natural resource managers. Forecasting approaches range from machine learning that is agnostic about underlying biological mechanisms to process-based models that incorporate mechanisms but are often complex and tailored toward specific species. Here we blend these approaches by constraining empirical dynamic modeling , a machine learning approach, with the metabolic theory of ecology (MTE). Focusing on short-lived ectotherms with high-frequency sampling, the conditions under which our methodology is likely to be most effective, we obtained improved forecasts for most time series. This lends support to the MTE as a general predictive theory and provides a new tool with which to forecast abundances in environments with seasonal and/or interannual temperature change.

Author contributions: S.B.M., T.L.R., C.C.S., D.A., and F.P. designed research; S.B.M., T.L.R., C.C.S., D.A., and F.P. performed research; S.B.M. contributed new analytic tools; S.B.M, T.L.R., and D.A. analyzed data; S.B.M., T.L.R., C.C.S., D.A., and F.P. contributed to the writing and revision of the paper; and S.B.M. and F.P. wrote the paper.

The authors declare no competing interest.

This article is a PNAS Direct Submission.

[1]To whom correspondence may be addressed. Email: steve.munch@noaa.gov or frank.pennekamp@ieu.uzh.ch.

This article contains supporting information online at https://www.pnas.org/lookup/suppl/doi:10.1073/pnas.2211758120/-/DCSupplemental.

Published March 17, 2023.

For biological systems, temperature stands out as a major driver of processes such as enzymatic reactions, growth, reproduction, body size, and the pace of life, resulting in well-described patterns such as latitudinal and altitudinal diversity gradients (15, 16). Seasonal temperature fluctuations can be large, and due to climate change, global temperatures are expected to rise and show increased variability within and across regions over the coming century (17, 18). Shifting temperatures are already influencing the population dynamics of a wide range of taxa (19, 20), including pest species (21) and harmful algae (22); however, our ability to forecast the population-dynamic consequences of increasing temperatures across a wide range of organisms is still in its infancy.

The metabolic theory of ecology (MTE) is one of the few mechanistic ecological theories emerging from biophysical first principles (15). The MTE posits that biological rates, such as resting metabolic rate or growth rates, allometrically scale with body mass (with an exponent of ¾) and for ectotherms, increase with temperature according to the Boltzmann factor (also known as the Arrhenius equation) $e^{-E/kT}$ (where E is the activation energy and corresponds to a value of 0.65, k is Boltzmann's constant and T is temperature in Kelvin) (15). Endotherms, which can maintain a relatively constant body temperature, are not expected to show this same scaling of rates with environmental temperature. The effects of body size and temperature on individuals subsequently scale up to determine population-level properties (e.g., intrinsic rate of growth, carrying capacity, rate of extinction, or mortality) (15, 23, 24), and ecosystem properties like net ecosystem respiration (25). The MTE has outstandingly synthesized patterns across a wide range of scales from cell division to individual metabolism to macro-ecology (15, 24, 26). However, most predictions of the MTE are for static, steady-state conditions.

The ability of the MTE to scale to higher-level processes suggests the theory could help forecast how temperature changes will affect population, community, and ecosystem dynamics. Indeed, models using the MTE have elucidated how population dynamic parameters scale with temperature (e.g., intrinsic rate of increase, carrying capacity, rate of extinction) (23, 24, 27, 28). The MTE has also successfully predicted within-host parasite dynamics across constant temperature environments (28). However, such detailed information on the temperature dependence of multiple vital rates is unavailable for most taxa, severely limiting our ability to forecast population dynamics under changing temperature conditions using mechanistic population models.

Here we blend EDM (a data-driven forecasting method) with the temperature dependence of the MTE to forecast population dynamics of a range of taxa under natural temperature fluctuations. Our predictive hybrid framework rescales time according to the MTE to achieve a constant "metabolic" time step: when temperatures are high, the metabolic time step encompasses less calendar time; when temperatures are low, it encompasses more calendar time (Fig. 1 *A* and *B*). Since empirically estimated activation energies deviate from the "universal" average value of 0.65 (29), the activation energy used for this rescaling can either be specified or estimated from the data. In keeping with ecosystem applications of the MTE (e.g., refs. 30 and 31), we assume that the effect of temperature is *separable* (see *Methods* for a more precise definition) from other influences on population dynamics. That is, temperature affects the overall rate of dynamics, not their form. Strictly speaking, this requires that all interacting species have similar thermal responses. Lack of separability could result from large variation in temperature dependence among interacting species and/or among different vital rates within a species. As an example, in a cyclic predator–prey system with separable temperature dependence, only the period of oscillations would change with temperature. As a counterexample, any system where a change in temperature causes a shift from oscillatory to equilibrium dynamics (e.g., ref. 32) would lack separability. However, when thermal responses are similar across the observed range of temperatures, though not identical, we expect EDM with MTE temperature dependence to improve prediction relative to standard EDM, despite the lack of strict separability. If, in contrast, the separability assumption is strongly violated, the method will not work, which will be apparent in the lack of improvement. We examined the reasonableness of the separability assumption using existing laboratory data and tested the robustness of the method to variation in temperature dependence using simulations.

Using a collection of empirical field time series, we compared the EDM Simplex projection algorithm using a fixed calendar time step (33) to Simplex projection using a metabolic time step. For the metabolic time step models, we used either the universal temperature dependence of 0.65 (the UTD model), temperature dependence estimated from the data (the MTE-EDM model), or for three species for which we could obtain data, temperature dependence based on empirical thermal performance curves (the TPC model). For comparison, we also fit

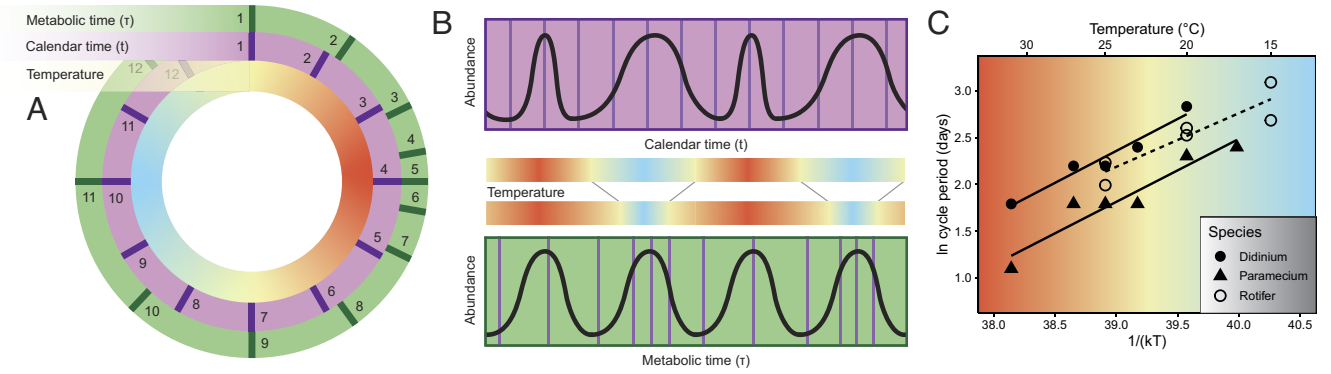

Fig. 1. Conceptual diagrams illustrating principles behind MTE-EDM and the rescaling of time with temperature. The example in *A* and *B* depicts a seasonal system. (*A*) Calendar time and metabolic time proceed at different rates depending on temperature (light blue indicates low temperatures, red high temperatures). (*B*) Abundance dynamics will proceed faster at higher temperatures, but have the same underlying dynamics when using a metabolic time step. A constant metabolic time step can be achieved using a dynamic calendar time step based on temperature. (*C*) Under the assumptions of MTE-EDM, population cycle period should decrease with increasing temperature. Consistent with this assumption, empirically measured cycle periods in constant-temperature laboratory experiments scale with temperature.

a calendar time step model with temperature as a covariate, which is a common alternative approach for incorporating temperature into EDM (34, 35).

Results

We first tested whether the temperature separability assumption is reasonable using data from published laboratory experiments measuring population dynamics across a gradient of constant temperatures. The pace of population dynamics, measured by log cycle period, displayed temperature scaling consistent with the MTE in three species (Fig. 1*C* and *SI Appendix*, Fig. S1 and Table S1). The scaling exponent for the rotifer *Brachionus calyciflorus* was 0.57 (95% CI: 0.22 to 0.93, $R^2 = 0.83$) (36), and exponents for the predator–prey pair *Didinium nasutum* and *Paramecium caudatum* were 0.68 (95% CI: 0.39 to 0.97, $R^2 = 0.95$) and 0.67 (95% CI: 0.37 to 0.97, $R^2 = 0.91$), respectively (37). However, we did not find the expected scaling relationship in two additional studies: a *Tetrahymena pyriformis-Pseudomonas fluorescens* predator–prey system (38) and the moth *Plodia interpunctella* (39). In the latter studies, temperature likely drove those systems across bifurcations that qualitatively changed their dynamics instead of only influencing the rate of change. Thus, while it is clear that not all systems meet the assumptions of MTE-EDM, for systems that do, we would expect the method to produce forecasting improvements in environments with temperature variation.

As a proof of concept, we simulated a chaotic three-species food chain (40) under two temperature change scenarios: a linear temperature increase (*SI Appendix*, Fig. S2*A*), and a more realistic scenario with seasonal temperature variation (26 °C), a long-term trend (~1.5 °C over 10 y), and stochasticity (Fig. 2*A*). In both scenarios, Simplex that does not account for temperature change results in poor predictive performance ($R^2 < 0.2$), even as the embedding dimension (number of lags used) was increased (Fig. 2*C* and *SI Appendix*, Fig. S1*C*). MTE-EDM greatly improved performance over Simplex ($R^2 > 0.8$, Fig. 2*C* and *SI Appendix*, Fig. S2*C*), and the use of the dynamic time step improved the resolution of the reconstructed underlying attractor, which was otherwise distorted by temperature-dependent dynamics (Fig. 2 *D* and *E* and *SI Appendix*, Fig. S1 *D* and *E*). These simulations also demonstrate the effectiveness of MTE-EDM when temperature is nonstationary and shows directional trends.

To explore the sensitivity of MTE-EDM to variation in species-specific responses to temperature, we ran additional multispecies simulations with variable numbers of interacting ecto- and endotherms, for which the ectotherms had variable activation energies (*SI Appendix*, Figs. S3 and S4). Although MTE-EDM is applied to data from a single species, the estimated activation energy integrates the temperature dependence of all closely interacting species, and variation in temperature dependence among species makes the population dynamics nonseparable from temperature. Results show that in ectotherm-dominated systems,

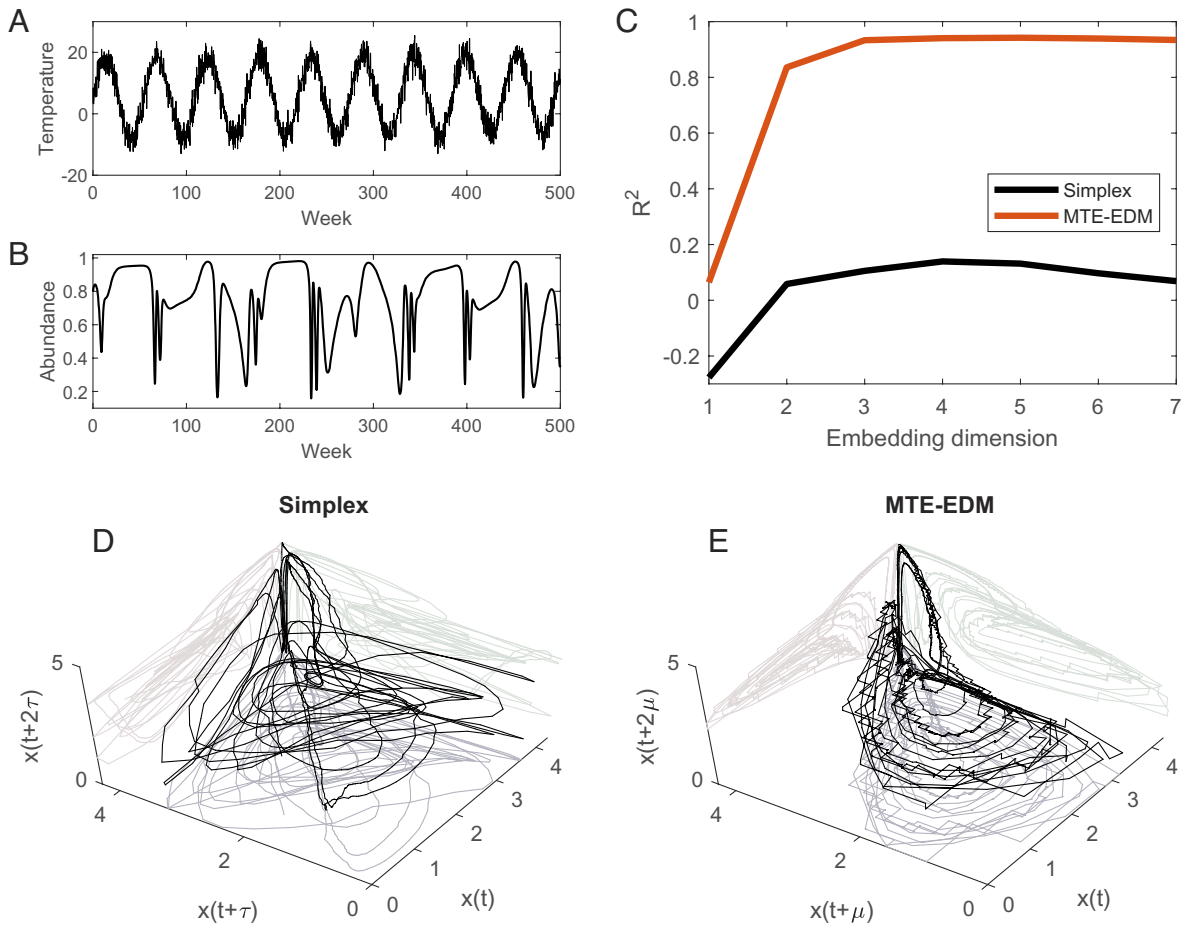

Fig. 2. Simulated population dynamics with temperature seasonality, a long-term trend, and stochasticity. Panel (*A*) shows temperature and (*B*) abundance time series. (*C*) Leave-one-out prediction R^2 for Simplex and MTE-EDM with different embedding dimensions. (*D*) Reconstructed attractor in delay coordinate space using a fixed calendar time step or (*E*) using a fixed metabolic time step.

MTE-EDM is robust to variation in activation energy, recovering the correct mean activation energy in the presence of considerable variation among species. MTE-EDM frequently outperformed Simplex, particularly as the mean activation energy increased and variability in the activation energy among species decreased. The exception, not surprisingly, was when most community members were endotherms, in which case the mean activation energy estimate was biased low, and performance did not improve notably over Simplex. Thus, the method is robust to modest violations of the assumption of strict separability.

We next evaluated whether MTE-EDM improves prediction in field populations exposed to natural temperature fluctuations. We assembled a database of 22 time series from eight locations (five aquatic, three terrestrial) spanning a range of taxa (e.g., phytoplankton, crustaceans, moths, rodents; Table 1 and *SI Appendix*, Table. S2). Sampling intervals ranged from half-weekly to monthly, and mean temperatures ranged from 9.8 to 26.7 °C. Absolute forecasting skill for both Simplex and MTE-EDM was high across time series, with R^2 values ranging from 0.22 to 0.85 (mean: 0.60) for Simplex and 0.39 to 0.88 (mean: 0.67) for MTE-EDM (Table 1). For 18 of 19 ectotherm time series, MTE-EDM outperformed Simplex, increasing forecast skill of these 18 series by 20% on average (19% across all series, Fig. 3*A*). Likelihood ratio tests indicated that this improvement was statistically significant in 17 of 19 cases. In terms of R^2 values, MTE-EDM outperformed UTD in all cases, and UTD outperformed Simplex in only 8 of 19 cases. Using temperature as a covariate outperformed Simplex in 14 cases, but outperformed MTE-EDM in only three cases. Estimated activation energies from MTE-EDM were within the range of values estimated in other studies (29) and did not approach the parameter bounds (Fig. 3*C* and *SI Appendix*, Fig. S5). As expected, MTE-EDM resulted in little forecast improvements for three endotherm time series (0.8% on average, Fig. 3*A*). The estimated activation energies for the endotherm series were close to 0, and the use of UTD decreased performance.

Seasonality was the dominant source of temperature variability in our field time series [trend: 0 to 2.8 °C $year^{-1}$ (median 0.04); seasonal range: 1.4 to 24 °C (median 19)], as is typical of temperatures throughout most of the world (41). Among ectotherms, the degree of improvement when using MTE-EDM was strongly related to the seasonality of the environment, with larger improvement in forecast skill in more variable environments (Fig. 3*B*). This is a sensible result: If there is little variation in temperature, there will also be little variation in the length of the metabolic time step, and thus the MTE-EDM model will be similar to Simplex.

Despite the MTE's success in explaining large-scale biological patterns in relation to environmental temperature, physiologists have pointed out that the MTE's monotonic increase of vital rates with temperature is unrealistic (29). Thermal performance curves (TPCs) are usually domed: Vital rates increase with temperature up to an optimum temperature and then decrease rapidly beyond the optimum (42). Organisms are typically exposed to a range of

Table 1. Metadata for empirical datasets used in the study and leave-one-out R^2 values for Simplex and MTE-EDM

Taxon		Location	Sampling interval	Time series length (n)	R^2 (Simplex)	R^2 (MTE-EDM)
Acartia hudsonica	copepod	Narragansett Bay	weekly	767	0.63	0.88
Acartia tonsa	copepod	Narragansett Bay	weekly	767	0.72	0.78
Phytoplankton		Lake Greifensee	monthly	388	0.57	0.57
Cyanobacteria		Lake Greifensee	monthly	388	0.58	0.61
Eukaryotes		Lake Greifensee	monthly	388	0.37	0.39
Bythotrephes longimanus	cladoceran	Lake Geneva	biweekly	1,038	0.85	0.86
Eudiaptomus gracilis	copepod	Lake Geneva	biweekly	1,038	0.78	0.78
Kellicottia longispina	rotifer	Lake Geneva	biweekly	1,038	0.83	0.84
Adoxophyes honmai	moth	Japan	5 d	2,754	0.54	0.62
Acartia sp., nauplii	copepod	Wadden Sea	weekly	503	0.48	0.65
Acartia sp., copepodites	copepod	Wadden Sea	weekly	503	0.51	0.63
Harpacticoida	copepod	Wadden Sea	weekly	503	0.66	0.68
Balanidae, nauplii	barnacle	Wadden Sea	weekly	503	0.66	0.74
Spionida, metatrochophora	polychaete	Wadden Sea	weekly	503	0.36	0.50
Temora longicornis, nauplii	copepod	Wadden Sea	weekly	503	0.58	0.70
Anarsia lineatella	moth	Greece	3 d	322	0.22	0.51
Adoxophyes orana	moth	Greece	3 d	322	0.43	0.45
Grapholita moleasta	moth	Greece	3 d	322	0.60	0.70
Zooplankton		Bermuda	biweekly	600	0.49	0.50
Dipodomys merriami	kangaroo rat	Portal, Arizona	monthly	312	0.80	0.80
Dipodomys ordii	kangaroo rat	Portal, Arizona	monthly	312	0.80	0.80
Onychomys torridus	mouse	Portal, Arizona	monthly	312	0.70	0.71

Data citations are in *SI Appendix*, Table S2.

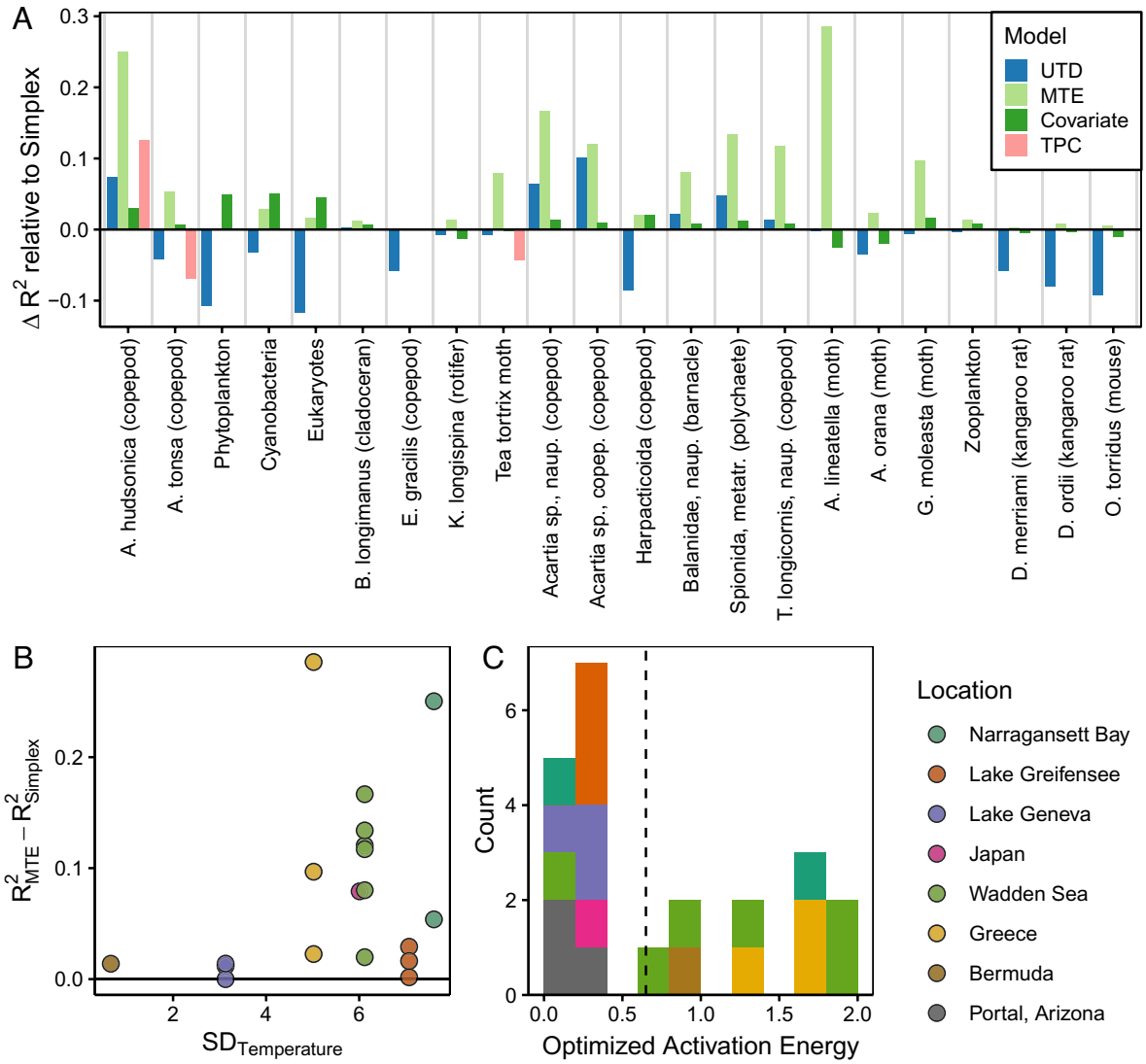

Fig. 3. (*A*) Change in forecast performance (as measured by change in leave-one-out prediction R^2) for each model relative to the Simplex, for each empirical time series. Models used a metabolic time step based on either universal temperature dependence (UTD), optimized temperature dependence (MTE), or empirical thermal performance curves (TPC), or used a calendar time step with temperature as a covariate (Covariate). Only three series had TPC models. Mean ± SD for change in R^2 across ectotherm series: UTD: −0.01 ± 0.06, MTE: 0.08 ± 0.08, Covariate: 0.01 ± 0.02. (*B*) Change in forecast performance (MTE vs. Simplex) vs. SD of temperature, excluding endotherms (3 rodent time series from Portal, Arizona). (*C*) Distribution of optimized activation energies from MTE-EDM. The vertical dashed line is the UTD value (0.65). The Simplex model (no temperature dependence) corresponds to an activation energy of 0. Exact activation energy values are given in *SI Appendix*, Fig. S5.

temperatures, including suboptimal temperatures, especially in seasonal environments (43). Our modeling framework can readily use a TPC instead of MTE temperature scaling to determine the length of the metabolic time step, which we expect to produce better results when the organism often experiences temperatures on the descending limb of the TPC. We obtained TPCs for the three species in our time series database for which curves were available and tested whether TPC-based models could improve forecasts. We found that forecasting skill was worse than MTE-EDM in all cases and worse than Simplex in two cases (Fig. 3*A*).

Discussion

Previous work on EDM has shown that unequally spaced lags can be optimal for modeling systems with multiple timescales (44) and that in "driven" systems, delays of the driver (in this case temperature) included as additional predictors (covariates) can improve the forecast performance (45). However, Takens' theorem (12) shows that adding lags of temperature to an EDM model also adds information from other variables that interact with temperature, making a mechanistic interpretation difficult. For instance, (35) found that the temperature dependence at lag 1 was unimodal or increasing (as expected for thermal performance) but was bowl-shaped or decreasing at lag 2, possibly representing an indirect effect through predation or competition. Here we show that constraining EDM to obey a known mechanism outperforms the covariate approach in the majority of cases. Additionally, using a metabolic time step adds only one degree of freedom to the model, and permits model comparison to Simplex with a simple likelihood ratio. In contrast, the change in degrees of freedom that results from adding temperature as an additional coordinate in the nonparametric Simplex model is difficult to determine a priori, rendering a likelihood ratio test inappropriate for comparing this model. Our study is the first demonstration that separable, nonautonomous dynamics can be embedded through a simple time scale change.

Not all biological rates or organisms have the same temperature dependence (29, 46, 47), and allowing for variable activation

energies improved performance over the universal value of 0.65. Surprisingly, MTE-EDM's temperature scaling performed better than scaling using empirical TPCs, despite the known unimodal shape of thermal performance (48). This could be because most temperatures experienced by the focal species were below the TPC optimum. Additionally, different biological processes have different TPCs (29), and the particular one measured may or may not reflect the temperature dependency of the population dynamics, which integrates across many biological processes and interacting species (49). However, since only three species had TPCs, more applications are needed before we can draw any general conclusions about the performance of this method relative to MTE-EDM.

Of course, temperature is not the only factor affecting biological rates or population dynamics, which may explain why MTE-EDM did not always greatly improve forecast skill, even with ample temperature variation. Understanding whether there are general rules for how temperature scaling shifts when resources are limiting is an active area of research, and testing whether the patterns described in the literature can be used as constraints to improve forecasts would be a useful direction for future forecasting research. For example, ecological stoichiometry posits that phosphorus content directly influences the growth rates of aquatic organisms (50). Ongoing efforts to expand the metabolic theory to include important constraints such as stoichiometry (e.g., refs. 50 and 51) could mean that additional adjustments to the metabolic time step may be possible [e.g., based on phosphorus availability (52)]. However, not all environmental factors influence biological rates in a known or universal way that is separable from other population dynamics, as assumed in MTE-EDM, so there is not necessarily a straightforward way to integrate them into the metabolic time step. In these cases, environmental variables could be covariates rather than constraints or indirectly captured by the time lags. Coupling EDMs with physical models is another approach to incorporating mechanism that has been recently explored. For instance, EDM has recently been used in a hybrid modeling approach where data-driven predictions of the biogeochemical components of Lake Geneva were combined with a model of lake physics to predict future lake health (53). This yielded better forecast performance for dissolved oxygen concentration than the physical model. Blending data-driven methods with theory therefore provides new avenues to both improve forecasts and increase our understanding of relevant mechanisms.

When using MTE-EDM, practitioners must consider the timescale of the system they are modeling and the resolution of the population and temperature data available. First, MTE-EDM needs samples taken frequently enough to be able to construct uniform metabolic time steps. Sampling intervals that are too coarse limit our ability to do so. Second, MTE-EDM requires sufficient temperature variation on timescales relevant to the focal organism. For example, in all of our field time series, the focal organisms all had relatively short generation times, often less than the annual temperature cycle, resulting in temperature variation across generations. In contrast, population dynamics of species with generation times >>1 y should be relatively insensitive to seasonal fluctuations in temperature because from one generation to the next, the mean temperature will be more or less the same. Long-lived species may be sensitive to interannual variation in temperature (including climate change), but since this variation is typically much less than seasonal temperature variation (e.g., ~2 °C over the past 100 y vs. 20 °C within a year), it may only be apparent over very long timescales. Hence, the effectiveness of MTE-EDM will depend on the generation time of the organism, the observed temperature range, and the availability of data. At present, we expect MTE-EDM to be most effective for ectotherms with short generation times (~1 y or less) and high-frequency sampling (at least monthly). That said, we note that the change of variables used here is generic—any driver with approximately separable effects on dynamics could be built into EDM in this way.

Although MTE-EDM improved forecasts in the series we analyzed and our simulations indicated that MTE-EDM is robust to modest variation in activation energy among interacting ectotherms, it is worth noting conditions under which MTE-EDM will not improve forecasts. MTE-EDM will not improve forecasts when there is little variation in temperature, or when most interacting species are insensitive to temperature (e.g., endotherms). Less obviously, MTE-EDM is not expected to work when the separability assumption is strongly violated (e.g., where vital rates within and across species have sufficiently different effects over the observed range of temperatures). In particular, it will not improve forecasts when the lack of separability results in temperature driven shifts in structural stability, as occurs in some models (30, 51), experimental systems (36), and field systems [e.g., tea tortrix moth (52)]. The prevalence of such temperature-driven bifurcations in natural systems under current climate conditions is an open question. On the other hand, in cases where the temperature does vary, a failure of MTE-EDM to improve performance over Simplex suggests that either the system is temperature-independent (activation energy near 0) or that nonseparability is present. So, although we do not expect the MTE-EDM approach to be useful in all systems, its failure suggests alternative hypotheses that are worth exploring.

Although we did not see this in our data and have insufficient sample size to draw any general conclusions, we suspect MTE-EDM might work better on aggregated time series, since species-specific temperature dependencies may average out. Aggregation has also been shown to lead to higher forecast accuracy with EDM (54).

EDM—and other data-driven approaches—are powerful tools for making predictions and gaining insights into complex systems. Their power comes from their generality—we do not need to know how a system works for them to be useful. However, one of the strengths of mechanistic model building is that known mechanisms and auxiliary data (not time series) are readily incorporated. Several previous studies have noted the importance of bringing together empirical and mechanistic approaches (8, 55–57). Our approach is a novel addition to this growing toolbox. For systems that meet the assumptions of the method, it offers a new way to account for temperature variability and nonstationarity both now and in a future increasingly influenced by climate change.

Materials and Methods

Time Delay Embedding. Time delay embedding refers to the reconstruction of system dynamics using time lags of one or more variables from that system. For a generic, autonomous dynamical system of dimension S,

$$dx_i / dt = f_i(x_1, \ldots, x_S), \quad [1]$$

that converges to an attractor with dimension $d < S$, Takens proved that the lag vectors $X_i(t) = \{ x_i(t), x_i(t - \tau), \ldots, x_i(t - E\tau) \}$ are sufficient to embed the attractor, where τ is a time delay and $E + 1$ is the embedding dimension (12). For the remainder, we do this for each time series independently and drop the subscript i to simplify the notation. The practical upshot of Takens' theorem is that we can model the next state, $x(t)$, as,

$$x(t) = F(x(t-\tau), \ldots, x(t-E\tau)), \quad [\mathbf{2}]$$

where one of several function approximation schemes can be used to estimate the delay embedding map, F, from time series data. The simplest such scheme is the nearest neighbor approach, referred to in ecology as the Simplex projection algorithm (33, 58). To make a prediction for $x(t)$, Simplex uses the averages of the $E+1$ nearest neighbors of $\{x(t-\tau), \ldots, x(t-E\tau)\}$. Although there have been many elaborations on this approach, Simplex makes the fewest assumptions and has the fewest tunable parameters. As such, it is a natural benchmark for generalization.

Rescaling Time with Temperature (Metabolic Embedding). The MTE posits that the effect of temperature (T) on metabolism structures fecundity and mortality rates, and hence species interactions. Within ectotherms, the activation energy is highly conserved. Under these assumptions, the population dynamics of the i th species are given approximately by,

$$dx_i / dt = f_i(x_1, \ldots, x_S, T) \approx f_i(x_1, \ldots, x_S)h(T), \quad [\mathbf{3}]$$

where $h(T)$ is the average temperature dependence and f_i describes the effects of all other state variables. This approximation assumes the population and temperature dynamics are separable, such that temperature primarily affects the overall rate of change, and that all species approximately adhere to the same universal temperature dependence. This is clearly not exactly true for most real systems and we evaluate the consequence of deviations using simulations.

System [**3**] falls under the skew-product embedding theorems of Stark (45), which would expand the delay coordinate space to include lags of temperature in a nonparametric way. This is the justification for using temperature as an additional coordinate (covariate) in the Simplex model. However, including temperature in this way does not explicitly take advantage of the known functional dependence on temperature, i.e., $h(T) = e^{-E_0/kT}$ where $k = 8.617 \times 10^{-5} eV / K$ is Boltzmann's constant, T is temperature in degrees Kelvin, and E_0 is the activation energy.

Here, we make use of both the separability implied by Eq. **3** and the fact that $h(T)$ is known, to introduce a metabolic time, μ, which renders the dynamics autonomous. Specifically, if $d\mu/dt = h(T)$, then $dx_i / d\mu = f_i(x_1, \ldots, x_S)$, eliminating the need for skew-product embedding. Integrating over a fixed μ -step, we obtain a discrete μ model,

$$x_{i,n} = F_i(x_{i,n-1}, \ldots, x_{S,n-1}),$$

where $x_{i,n} = x_i(t_n)$ and the times t_n are defined implicitly by $\int_0^{t_n} h(T) = n\mu$. From here, Takens theorem allows us to re-cast the dynamics as,

$$x_n = \tilde{F}(x_{n-1}, x_{n-2}, \ldots, x_{n-E})$$

where we have again dropped the subscript i to simplify the notation though we remind the reader that the inputs to $\tilde{F}$ are lags of a single-state variable.

If data were available in continuous time, we would construct delay vectors for each $x(t_n)$ such that $\int_{t_{n-j}}^{t_n} h(T)dt = j\mu$ exactly. In practice, however, data are available on a discrete time step so some approximation is necessary. For simplicity, we find the sampling times t_{n-j} such that $\sum_{i_{n-j}}^{t_n} h(T_i)\Delta t$ is as close to $j\mu$ as possible. Given the collection of metabolic delay vectors, we use the same nearest-neighbor averaging to approximate F that we used for the Simplex algorithm.

Although $E_0 = 0.65$ has been referred to as "universal temperature dependence" (UTD) (15), subsequent meta-analyses (29) found substantial variability in E_0 across species and traits. For MTE-EDM, we, therefore, estimate E_0 by computing the log likelihood on a grid of 50 values of E_0 from 0 to 2 and a maximum embedding dimension of 15. In keeping with other EDM studies that minimize squared prediction errors, a Gaussian likelihood was used. Note that UTD ($E_0 = 0.65$) and Simplex ($E_0 = 0$) are special cases of MTE-EDM, so that twice the log likelihood ratio is expected to follow a chi-square distribution with one degree of freedom. It is less clear how the degrees of freedom change when using temperature as an additional coordinate, so significance levels for a likelihood ratio test would be approximate in this case. Although MTE-EDM is applied to data for a single species, it is important to recognize that the estimated E_0 represents an average for the species with which it closely interacts, rather than a species-specific metabolic rate.

Simulated Data. As a proof of concept, we simulated a chaotic three-species food chain (40) in which the vital rates depend on temperature as in Eq. **3**. Specifically, we used,

$$\frac{dx}{dt} = h(T)\left[\frac{x(1-x) - axy}{(1+bx)}\right],$$

$$\frac{dy}{dt} = h(T)\left[\frac{axy}{(1+bx)} - \frac{cyz}{(1+dy) - my}\right],$$

$$\frac{dz}{dt} = h(T)\left[\frac{cyz}{(1+dy) - \mu z}\right],$$

where $a = 5.0, b = 3.0, c = 0.1, d = 2.0, m = 0.4, \mu = 0.01$ and the initial conditions were $x(0) = 0.8, y(0) = 0.1, z(0) = 9.0$. The system was integrated using a 4th order Runge-Kutta scheme on a weekly time step for 500 wk. To provide interesting test cases, we simulated a temperature trend, $T(t) = 0.052t - 8$, and a more realistic scenario with seasonal temperature variation, a long-term trend, and stochasticity, $T(t) = 5 + 13\sin(2\pi t / 55) + 0.003t + 2.6\in(t)$ where $\in(t) \sim N(0, 1)$ is white noise. The linear increase of 0.003 °C wk^{-1} results in a net increase of 1.5 °C over the ~10-y simulation.

To understand the effect of variable activation energies within a community, we also simulated 10 y of weekly data using the food chain model described above, but with $h(T)$ allowed to vary among species–violating the assumption of strict system-level separability. We considered four scenarios: 1) two ectotherms, 2) three ectotherms, 3) two ectotherms and one endotherm, and 4) one ectotherm and two endotherms. For each ectotherm, we generated random activation energies drawn from a Gaussian distribution with different means (0.20, 0.32, 0.65, 1.20) representing most of the typically observed range crossed with three levels of variability (SD: 0, 0.1, 0.2). Note that the interval 0.2 to 1.2 was originally proposed for variation in activation energy (26) and provided good bounds for within-species variation in lifespan (59), while 0.32 and 0.65 are typical values for photosynthesis and ectotherm metabolism, respectively.

For each of the four scenarios, four mean activation energies, and three SDs, we ran 50 replicates from random initial conditions for a total of 2,400 simulated datasets. For each dataset, we used the MTE-EDM approach to estimate the activation energy and used likelihood ratio tests to assess the probability that MTE-EDM would be significantly better than Simplex.

Analysis of Empirical Data.

Cycle period in laboratory experiments. To examine the impact of temperature on population cycle period, we searched the literature for laboratory experiments reporting population dynamics at different constant temperatures. This search yielded four studies: a rotifer (*B. calyciflorus*) population (36), a ciliate (*Didinium-Paramecium*) predator-prey system (37), a moth (*P. interpunctella*) (39), and a ciliate-bacteria (*T. pyriformis-P. fluorescens*) predator–prey system (38). Raw data were obtained from supplementary materials or, if necessary, directly from figures using WebPlotDigitizer (60).

We used spectral analysis to assess the periodicity for each abundance time series. To compute the power spectrum, we used penalized (ridge) regression onto sine and cosine basis functions with frequencies $2\pi s/N$, where $s = 2, 3, \ldots, N/2$ and N is the time series length (thus, the longest period considered was $0.5N$, and the shortest was two time steps). Time series were rescaled to mean 0 and unit variance prior to analysis, and the penalty was set to 0.01. Power at each frequency was calculated from the sine and cosine coefficients. The frequency (cycle period) with the highest power was then selected. For (38), we performed analyses on the average abundance at each time point and excluded replicate A for *T. pyriformis* because the density was 0 throughout the time series. For ref. 37, visual inspection of the time series showed that *Didinium* and *Paramecium* each went through one cycle before going extinct. Thus, we computed cycle period as the length of time to extinction. The *Didinium* population at 17 °C did not finish its cycle (i.e., it did not go extinct) during the experiment, so was excluded.

We performed ordinary least squares regression to assess the relationship between natural log-transformed cycle period and inverse absolute temperature,

i.e., $1/kT$, where k is Boltzmann's constant. The slope of this relationship corresponds to the activation energy.

Natural population dynamics. To evaluate the MTE temperature effect on natural populations, we assembled a database of time series from 22 short-lived species from terrestrial and aquatic environments (Table 1 and *SI Appendix*, Table S2). We chose to focus on species with subannual sampling intervals and short generation times in order to encompass seasonal variation in temperature and ensure sufficient data to reconstruct dynamics. Most time series were species level, although four time series represented species aggregates (e.g., phytoplankton). Sampling intervals ranged from 3 d to 1 mo, and sampling time ranged from 2 to 40 y. Temperature data were either recorded during sample collection or obtained from nearby sources (*SI Appendix*, Table S2). If a database contained multiple species, for our proof-of-concept purposes, we analyzed the 5 to 6 most abundant species with the longest continuous records. We also excluded series if the Simplex algorithm had prediction R^2 less than 0.2.

Each abundance time series was square-root–transformed and standardized to zero mean and unit SD prior to analysis. Since the sampling interval was somewhat variable for many of the time series, series were interpolated to the shortest constant interval (3 d, weekly, biweekly, or monthly) that was most consistent with the original sampling scheme using a Gaussian process regression with a cyclic prior mean with Fourier modes at 2^s y where $s = -2, -1, 0, 1, 2, 3$. Temperature data were interpolated similarly, but were not square-root–transformed.

For each time series, we fit two calendar time step models (standard Simplex, temperature as a covariate), and two metabolic time step models (UTD, MTE-EDM). For the calendar time step models, we selected the pair of embedding dimension and time delay, τ, that maximized forecast accuracy: We evaluated embedding dimensions ranging from 1 to 5, and time delays ranging from 1 to 12 steps, where the step size was set by the original sampling scheme. For the metabolic time step models, we selected the embedding dimension that maximized forecast accuracy, fixing the metabolic delay, μ, to the average metabolism over the same time step. That is, if the time series was sampled weekly, for a total of N weeks, we set $\mu = \frac{1}{N}\sum_i e^{-E_0/kT_i}$. Forecast accuracy was measured using leave-one-out prediction R^2, excluding the time point before and after, which was also used as our measure of forecast performance. While alternative cross-validation schemes or performance measures may give different results in terms of absolute forecast skill, the relative performance of the different models should be the same.

To evaluate the effect of thermal performance curve (TPC) shape on metabolic embedding, we obtained empirical TPCs for two copepod species (*Acartia tonsa*, *Acartia hudsonica*) and the tea tortrix moth (*Adoxophyes honmai*). TPCs for the copepods were obtained by fitting a Sharpe–Schoolfield model (61) to egg production data for each copepod species (62). For *Adoxophyes honmai,* we fit the same model to laboratory data for lifetime production of hatching eggs, calculated from data for age-specific survival, fecundity, and egg hatchability (63). TPCs were unavailable for the other species for which we had time series.

Data, Materials, and Software Availability. No new data were used. Laboratory data sources are cited in the main text; field data sources are listed in *SI Appendix*, Table S2. The laboratory time series, interpolated field time series, and all code required to reproduce the analyses are available at https://doi.org/10.5281/zenodo.7682553 (64). The datasets used for Lake Geneva are © OLA-IS, AnaEE-France, INRAE of Thonon-les-Bains, CIPEL, citation in *SI Appendix*, Table S2.

ACKNOWLEDGMENTS. The University of Zurich Research Priority Program on Global Change and Biodiversity supported this research. We thank the two anonymous reviewers for their constructive comments and suggestions, which have considerably improved the methodology and manuscript. F.P. was supported by the Swiss NSF (grant 310030_197811). C.C.S. was supported by a Hellman Fellowship Award at the University of California, Irvine. The scientific results and conclusions, as well as any views or opinions expressed herein, are those of the author(s) and do not necessarily reflect the views of NOAA or the Department of Commerce.

Author affiliations: [a]Southwest Fisheries Science Center, National Marine Fisheries Service, National Oceanic and Atmospheric Administration, Santa Cruz, CA 95060; [b]Department of Applied Mathematics, University of California, Santa Cruz, CA 95060; [c]Department of Ecology and Evolutionary Biology, University of California, Irvine, CA 92697; [d]Department of Zoology, University of British Columbia, Vancouver, BC V6T 1Z4, Canada; and [e]Department of Evolutionary Biology and Environmental Studies, University of Zurich, Zurich 8057, Switzerland

1. M. C. Dietze *et al.*, Iterative near-term ecological forecasting: Needs, opportunities, and challenges. *Proc. Natl. Acad. Sci. U.S.A.* **115**, 1424–1432 (2018).
2. J. S. Clark *et al.*, Ecological forecasts: An emerging imperative. *Science* **293**, 657–660 (2001).
3. D. E. Schindler, R. Hilborn, Prediction, precaution, and policy under global change. *Science* **347**, 953–954 (2015).
4. S. L. Brunton, J. L. Proctor, J. N. Kutz, Discovering governing equations from data by sparse identification of nonlinear dynamical systems. *Proc. Natl. Acad. Sci. U.S.A.* **113**, 3932–3937 (2016).
5. J. Elith, J. R. Leathwick, Species distribution models: Ecological explanation and prediction across space and time. *Annu. Rev. Ecol. Evol. Syst.* **40**, 677–697 (2009).
6. O. L. Petchey *et al.*, The ecological forecast horizon, and examples of its uses and determinants. *Ecol. Lett.* **18**, 597–611 (2015).
7. L. Parrott, Hybrid modelling of complex ecological systems for decision support: Recent successes and future perspectives. *Ecol. Inform.* **6**, 44–49 (2011).
8. M. Reichstein *et al.*, Deep learning and process understanding for data-driven Earth system science. *Nature* **566**, 195–204 (2019).
9. M. Alber *et al.*, Integrating machine learning and multiscale modeling–Perspectives, challenges, and opportunities in the biological, biomedical, and behavioral sciences. *Npj Digit. Med.* **2**, 1–11 (2019).
10. H. Ye, G. Sugihara, Information leverage in interconnected ecosystems: Overcoming the curse of dimensionality. *Science* **353**, 922–925 (2016).
11. H. Ye *et al.*, Equation-free mechanistic ecosystem forecasting using empirical dynamic modeling. *Proc. Natl. Acad. Sci. U.S.A.* **112**, E1569–E1576 (2015).
12. F. Takens, "Detecting strange attractors in turbulence" in *Dynamical Systems and Turbulence, Warwick 1980, Lecture Notes in Mathematics*, D. Rand, L.-S. Young, Eds. (Springer, Berlin, Heidelberg, 1981), pp. 366–381.
13. C. T. Perretti, S. B. Munch, G. Sugihara, Model-free forecasting outperforms the correct mechanistic model for simulated and experimental data. *Proc. Natl. Acad. Sci. U.S.A.* **110**, 5253–5257 (2013).
14. C. Karakoç, A. T. Clark, A. Chatzinotas, Diversity and coexistence are influenced by time-dependent species interactions in a predator–prey system. *Ecol. Lett.* **23**, 983–993 (2020).
15. J. H. Brown, J. F. Gillooly, A. P. Allen, V. M. Savage, G. B. West, Toward a metabolic theory of ecology. *Ecology* **85**, 1771–1789 (2004).
16. B. A. Hawkins *et al.*, A global evaluation of metabolic theory as an explanation for terrestrial species richness gradients. *Ecology* **88**, 1877–1888 (2007).
17. M. Collins *et al.*, "Long-term climate change: Projections, commitments and irreversibility" in *Climate Change 2013: The Physical Science Basis. IPCC Working Group I Contribution to AR5*, IPCC, Eds. (Cambridge University Press, Cambridge, 2013), pp. 1029–1136.
18. G. A. Meehl, C. Tebaldi, More intense, more frequent, and longer lasting heat waves in the 21st century. *Science* **305**, 994–997 (2004).
19. A. J. Davis, L. S. Jenkinson, J. H. Lawton, B. Shorrocks, S. Wood, Making mistakes when predicting shifts in species range in response to global warming. *Nature* **391**, 783–786 (1998).
20. E. Post, M. C. Forchhammer, Synchronization of animal population dynamics by large-scale climate. *Nature* **420**, 168–171 (2002).
21. K. J. Haynes, A. J. Allstadt, D. Klimetzek, Forest defoliator outbreaks under climate change: Effects on the frequency and severity of outbreaks of five pine insect pests. *Glob. Change Biol.* **20**, 2004–2018 (2014).
22. M. L. Wells *et al.*, Harmful algal blooms and climate change: Learning from the past and present to forecast the future. *Harmful Algae* **49**, 68–93 (2015).
23. V. M. Savage, J. F. Gillooly, J. H. Brown, G. B. West, E. L. Charnov, Effects of body size and temperature on population growth. *Am. Nat.* **163**, 429–441 (2004).
24. J. R. Bernhardt, J. M. Sunday, M. I. O'Connor, Metabolic theory and the temperature-size rule explain the temperature dependence of population carrying capacity. *Am. Nat.* **192**, 687–697 (2018).
25. G. Yvon-Durocher *et al.*, Reconciling the temperature dependence of respiration across timescales and ecosystem types. *Nature* **487**, 472–476 (2012).
26. J. F. Gillooly, J. H. Brown, G. B. West, V. M. Savage, E. L. Charnov, Effects of size and temperature on metabolic rate. *Science* **293**, 2248–2251 (2001).
27. C. F. Clements, B. Collen, T. M. Blackburn, O. L. Petchey, Effects of directional environmental change on extinction dynamics in experimental microbial communities are predicted by a simple model. *Oikos* **123**, 141–150 (2014).
28. D. Kirk *et al.*, Empirical evidence that metabolic theory describes the temperature dependency of within-host parasite dynamics. *PLOS Biol.* **16**, e2004608 (2018).
29. A. I. Dell, S. Pawar, V. M. Savage, Systematic variation in the temperature dependence of physiological and ecological traits. *Proc. Natl. Acad. Sci. U.S.A.* **108**, 10591–10596 (2011).
30. J. R. Schramski, A. I. Dell, J. M. Grady, R. M. Sibly, J. H. Brown, Metabolic theory predicts whole-ecosystem properties. *Proc. Natl. Acad. Sci. U.S.A.* **112**, 2617–2622 (2015).
31. B. J. Enquist *et al.*, Scaling metabolism from organisms to ecosystems. *Nature* **423**, 639–642 (2003).
32. M. Lindmark, J. Ohlberger, M. Huss, A. Gårdmark, Size-based ecological interactions drive food web responses to climate warming. *Ecol. Lett.* **22**, 778–786 (2019).
33. G. Sugihara, R. M. May, Nonlinear forecasting as a way of distinguishing chaos from measurement error in time series. *Nature* **344**, 734–741 (1990).
34. E. R. Deyle *et al.*, Predicting climate effects on Pacific sardine. *Proc. Natl. Acad. Sci. U.S.A.* **110**, 6430–6435 (2013).
35. T. L. Rogers, S. B. Munch, Hidden similarities in the dynamics of a weakly synchronous marine metapopulation. *Proc. Natl. Acad. Sci. U.S.A.* **117**, 479–485 (2020).
36. U. Halbach, Population dynamics of rotifers and its consequences for ecotoxicology. *Hydrobiologia* **109**, 79–96 (1984).

37. J. P. DeLong, S. Lyon, Temperature alters the shape of predator–prey cycles through effects on underlying mechanisms. *PeerJ* **8**, e9377 (2020).
38. K. E. Fussmann, F. Schwarzmüller, U. Brose, A. Jousset, B. C. Rall, Ecological stability in response to warming. *Nat. Clim. Change* **4**, 206–210 (2014).
39. A. M. Laughton, R. J. Knell, Warming at the population level: Effects on age structure, density, and generation cycles. *Ecol. Evol.* **9**, 4403–4420 (2019).
40. A. Hastings, T. Powell, Chaos in a three-species food chain. *Ecology* **72**, 896–903 (1991).
41. G. Wang, M. E. Dillon, Recent geographic convergence in diurnal and annual temperature cycling flattens global thermal profiles. *Nat. Clim. Change* **4**, 988–992 (2014).
42. M. J. Angilletta, *Thermal Adaptation: A Theoretical and Empirical Synthesis* (OUP Oxford, 2009).
43. T. L. Martin, R. B. Huey, Why "suboptimal" is optimal: Jensen's inequality and ectotherm thermal preferences. *Am. Nat.* **171**, E102–E118 (2008).
44. K. Judd, A. Mees, Embedding as a modeling problem. *Phys. Nonlinear Phenom.* **120**, 273–286 (1998).
45. J. Stark, Delay embeddings for forced systems. I. Deterministic forcing. *J. Nonlinear Sci.* **9**, 255–332 (1999).
46. A. C. Iles, Towards predicting community level effects of climate: Relative temperature scaling of metabolic and ingestion rates. *Ecology* **95**, 2657–2668 (2014), 10.1890/13-1342.1.
47. N. J. B. Isaac, C. Carbone, Why are metabolic scaling exponents so controversial? Quantifying variance and testing hypotheses. *Ecol. Lett.* **13**, 728–735 (2014).
48. G. Englund, G. Öhlund, C. L. Hein, S. Diehl, Temperature dependence of the functional response. *Ecol. Lett.* **14**, 914–921 (2011).
49. A. Gårdmark, M. Huss, Individual variation and interactions explain food web responses to global warming. *Philos. Trans. R. Soc. B Biol. Sci.* **375**, 20190449 (2020).
50. J. J. Elser *et al.*, Biological stoichiometry from genes to ecosystems. *Ecol. Lett.* **3**, 540–550 (2000).
51. A. P. Allen, J. F. Gillooly, Towards an integration of ecological stoichiometry and the metabolic theory of ecology to better understand nutrient cycling. *Ecol. Lett.* **12**, 369–384 (2009).
52. J. F. Gillooly, E. L. Charnov, G. B. West, V. M. Savage, J. H. Brown, Effects of size and temperature on developmental time. *Nature* **417**, 70 (2002).
53. E. R. Deyle *et al.*, A hybrid empirical and parametric approach for managing ecosystem complexity: Water quality in Lake Geneva under nonstationary futures. *Proc. Natl. Acad. Sci. U.S.A.* **119**, e2102466119 (2022).
54. V. Agarwal, C. C. James, C. E. Widdicombe, A. D. Barton, Intraseasonal predictability of natural phytoplankton population dynamics. *Ecol. Evol.* **11**, 15720–15739 (2021).
55. G. Sugihara *et al.*, Residual delay maps unveil global patterns of atmospheric nonlinearity and produce improved local forecasts. *Proc. Natl. Acad. Sci. U.S.A.* **96**, 14210–14215 (1999).
56. J. T. Thorson, K. Ono, S. B. Munch, A Bayesian approach to identifying and compensating for model misspecification in population models. *Ecology* **95**, 329–341 (2014).
57. J. Runge *et al.*, Inferring causation from time series in Earth system sciences. *Nat. Commun.* **10**, 2553 (2019).
58. J. D. Farmer, J. J. Sidorowich, Predicting chaotic time series. *Phys. Rev. Lett.* **59**, 845–848 (1987).
59. S. B. Munch, S. Salinas, Latitudinal variation in lifespan within species is explained by the metabolic theory of ecology. *Proc. Natl. Acad. Sci. U.S.A.* **106**, 13860–13864 (2009).
60. A. Rohatgi, WebPlotDigitizer (Version 4.6, Pacifica, California, 2020). https://automeris.io/WebPlotDigitize.
61. R. M. Schoolfield, P. J. H. Sharpe, C. E. Magnuson, Non-linear regression of biological temperature-dependent rate models based on absolute reaction-rate theory. *J. Theor. Biol.* **88**, 719–731 (1981).
62. B. K. Sullivan, L. T. McManus, Factors controlling seasonal succession of the copepods Acartia hudsonica and A. tonsa in Narragansett Bay, Rhode Island: Temperature and resting egg production. *Mar. Ecol. Prog. Ser.* **28**, 121–128 (1986).
63. F. H. Nabeta, M. Nakai, Y. Kunimi, Effects of temperature and photoperiod on the development and reproduction of *Adoxophyes honmai* (Lepidoptera: Tortricidae). *Appl. Entomol. Zool.* **40**, 231–238 (2005).
64. S.B. Munch, T. L. Rogers, D. Anderson, Integration of Metabolic Theory of Ecology and Empirical Dynamic Modeling (MTE-EDM). *Zenodo*. https://doi.org/10.5281/zenodo.7682553. Deposited 27 February 2023.